ELSEVIER

Journal of Molecular Catalysis B: Enzymatic 16 (2001) 7–15

JOURNAL OF MOLECULAR CATALYSIS B: ENZYMATIC

www.elsevier.com/locate/molcatb

Kinetic mechanism of β-xylosidase from *Trichoderma reesei* QM 9414

María Gómez, Pablo Isorna, Marta Rojo, Pilar Estrada*

Departamento de Bioquímica y Biología Molecular I, Facultad de Biología, Universidad Complutense, Ciudad Universitaria, 28040 Madrid, Spain

Received 24 October 2000; received in revised form 15 May 2001

Abstract

β-Xylosidase is a key enzyme in the hydrolysis of xylobiose to D-xylose. The enzyme was purified from cultures of *Trichoderma reesei* QM 9414 grown on wheat straw as a carbon source. β-Xylosidase shows the highest catalytic efficiency towards xylobiose and the highest affinity for 4-methylumbellyferyl-β-D-xylopyranoside, an arylxyloside whose aglycone is very hydrophobic. Studies of inhibition by products on the *p*-nitrophenyl-β-D-xylopyranoside kinetics and by an alternative product, 4-methylumbelliferone, supports an Ordered Uni Bi mechanism for the reaction catalysed by β-xylosidase. Competitive inhibition by a product analog, D-glucono-1,5-lactone is also compatible with the proposed mechanism.

Keywords: β-Xylosidase; Glycosidase; Mechanism; Kinetics

1. Introduction

Hydrolysis of xylan plays an important role in the breakdown process of plant material in nature since xylan is the major hemicellulose component in plant cell walls and the most abundant polysaccharide after cellulose [1]. The filamentous fungus *Trichoderma reesei* produces extracellular enzymes which degrade xylan into monomers. The major components of this xylanolytic system are endoxylanase (1,4-β-D-xylan-xylanohydrolase; EC 3.2.1.8) which hydrolyses the β-1,4 bonds in the main chain generating a mixture of xylo-oligosaccharides and β-xylosidase (1,4-β-D-xylan-xylohydrolase; EC 3.2.1.37) which cleaves off the terminal xylose units from the non-reducing end of xylo-oligosaccharides and is rate-limiting in xylan hydrolysis [2].

The catalytic mechanisms of enzymes that hydrolyse glycosides have been studied for several years [3–5] leading to classify them into two groups, those hydrolysing the glycosidic bond with net inversion of anomeric configuration and those doing so with net retention. Inverting glycosidases operate via a direct displacement of the leaving group by water whereas retaining ones utilize a double-displacement mechanism involving a glycosyl-enzyme intermediate. Despite these differences, both classes of glycosidases employ a pair of carboxylates at the active site, operate via transition states with substantial oxocarbenium ion character [6] and it is known that inverting enzymes never catalyse *trans*-glycosidation reactions [7].

Abbreviations: E, free enzyme; GL, D-glucono-1,5-lactone; MU, 4-methylumbelliferone; MUX, 4-methylumbelliferyl-β-D-xylopyranoside; *p*NPA, *p*-nitrophenyl-α-L-arabinofuranoside; *p*NP, *p*-nitrophenol; *p*NPX, *p*-nitrophenyl-β-D-xylopyranoside

*Corresponding author. Tel.: +34-91-3944620; fax: +34-91-3944672.
E-mail address: estrada@solea.quim.ucm.es (P. Estrada).

1381-1177/01/$ – see front matter
PII: S1381-1177(01)00038-8

The β-xylosidase from *Trichoderma reesei* is able to catalyse hydrolysis mainly of xylo-oligomers and aryl β-D-xylopyranosides, but also of α-L-arabinofuranosides [8,9]. Moreover, *Trichoderma reesei* β-xylosidase shows *trans*-xylosidation activity [10] and its aminoacid sequence has been aligned with the one of the β-glucosidase enzymes secreted by the same fungus (family 3). It does not show similarity with other β-xylosidases classified in families 39, 43 or 52 [8]. Despite numerous studies on β-xylosidase, no use has been made of steady-state kinetics to establish its kinetic mechanism, that is, to determine if the release of the reaction products is ordered.

We have studied the production of cellulolytic enzymes by the fungus *Trichoderma reesei* QM 9414 grown on wheat straw as sole carbon source [11] and determined the kinetic [12] and chemical mechanism [13] of the β-glucosidase it secreted. We have also purified the β-xylosidase produced by the fungus [14] and partially purified fractions of the enzyme have been immobilized on nylon powder [15]. The present paper investigates the kinetic mechanism of β-xylosidase by examining its kinetic behavior towards xylobiose and arylxylosides and the effects of reaction products, alternative product or a dead-end inhibitor on *p*-nitrophenyl-β-D-xylopyranoside hydrolysis.

2. Materials and methods

2.1. Materials

Xylobiose, D-xylose, *p*-nitrophenyl-β-D-xylopyranoside, *p*-nitrophenyl-α-L-arabinofuranoside, 4-methylumbelliferone, 4-methylumbelliferyl-β-D-xylopyranoside, bovine serum albumin, 3,5-dinitrosalycilic acid and D-glucono-1,5-lactone were from Sigma (Spain). *p*-Nitrophenol was from Fluka (Switzerland). DEAE-sepharose CL-6B was from Pharmacia (Sweden) and Ultrogel AcA 44 was from LKB (Sweden). Acetonitrile HPLC grade was from Scharlau (Spain) and all other reagents were of analytical grade from Merck (Germany).

2.2. Enzyme purification

Trichoderma reesei QM 9414 was cultured on wheat straw as previously described [11]. β-Xylosidase was purified from culture supernatant following the same procedure described for β-glucosidase purification [12] including ammonium sulfate precipitation, DEAE-Sepharose CL-6B and Ultrogel AcA 44 cromatographies. Purification to homogeneity of β-xylosidase was achieved after the gel filtration step, the fractions corresponding to the top of the elution peak were pooled and employed for determining the kinetic mechanism. SDS-PAGE of these fractions showed a single band [14]. Also, a replica gel containing the substrate (*p*NPX) was incubated with a non-denaturing PAGE of the fractions and showed a single yellow spot when treated with NaOH thereafter, indicating *p*-nitrophenol release demonstrating that only one catalytic species has activity against β-xylosides [14].

2.3. Analytics

Protein was measured according to Lowry et al. [16]. Bovine serum albumin was used as standard.

Reducing sugars were measured by the dinitrosalicylic reagent method [17] recording the absorbance of the reduced reagent at 530 nm in a Beckman DU-70 spectrophotometer. D-xylose was employed as a standard.

The actual D-glucono-1,5-lactone and D-gluconic acid content of 160 and 200 mM D-glucono-1,5-lactone solutions in standard buffer was determined by polarimetry. Freshly prepared samples of 1 ml and samples after remaining 30 and 60 min at room temperature were introduced in the glass cell (1 dm length) of a Perkin-Elmer 241 polarimeter thermostatized at 20°C and equipped with a sodium lamp (D, $\lambda = 589$ nm). The extent of rotation was measured, the specific rotation (α) was calculated as described [18] and the concentration of gluconic acid (c_{ga}) and of D-1,5-gluconolactone (c_{gl}) calculated by using Eq. (1):

$$c_{ga} \times \alpha_{ga} + c_{gl} \times \alpha_{gl} = \alpha \quad (1)$$

where α_{ga} is the specific rotation of D-gluconic acid and α_{gl} the specific rotation of the D-glucono-1,5-lactone at 20°C and 589 nm and summarized in the Merck Index [19].

2.4. Enzymatic assays

Controls of non-enzymatic hydrolysis were carried out routine for each substrate concentration and the

corresponding absorbance was subtracted from the absorbance measured in enzymatic assay tubes.

2.4.1. With p-nitrophenyl-β-D-xylopyranoside (pNPX)

β-Xylosidase activity was routinely assayed in incubation mixtures containing 10.6 μg protein and 3 mM *p*NPX in 1 ml 0.1 M sodium citrate buffer pH 4.0 (standard buffer) at 55°C for 10 min in a water bath. The enzymatic assay began when the enzyme was added to the tubes. The release of *p*-nitrophenol (*p*NP) was measured at 400 nm after the addition of 1 ml 0.4 M NaOH.

2.4.2. With p-nitrophenyl-α-L-arabinofuranoside (pNPA)

Enzymatic assays were carried out as described for *p*NPX.

2.4.3. With 4-methylumbelliferyl-β-D-xylopyranoside (MUX)

An amount of 2.65 μg protein were incubated with 1.5 mM MUX at 55°C for 10 min in 1 ml of 0.1 M citrate buffer pH 4.0. The reaction was stopped by the addition of 4 ml 0.2 M Gly/NaOH buffer pH 10.2 to surpass the pK_a of the 4-methylumbelliferone (MU) released which was measured in a Fluorescence Spectrophotometer Perkin-Elmer MPF-44E at $\lambda_{EX} = 360 \pm 3.5$ nm and $\lambda_{EM} = 455 \pm 2.5$ nm. MU was employed as a standard.

2.4.4. With xylobiose

Assays were carried out in 100 μl of standard buffer containing 76 μg protein and 3 mM xylobiose at 55°C for 20 min. The reaction was terminated by addition of 150 μl of dinitrosalicylic reagent, samples were boiled for 10 min and analysed for reducing sugars.

When *p*NP was employed as inhibitor on the *p*NPX kinetics, the amount of xylose produced could not be measured as reducing sugars since the remaining substrate was hydrolysed through boiling with the dinitrosalicylic reagent, thus, masking the enzymatic release. Therefore, xylose was analysed in the reaction mixture by HPLC (Merck Hitachi) employing a Kromasil Amino AV 603 column (250 mm × 4.6 mm from Analisis Vinicos). The HPLC system was equipped with a light scattering detector SEDEX 55 (45°C, 2 bar). The mobile phase was acetonitrile/water (75:25, v/v) with a flow rate of 2 ml/min. The retention time (t_R) of *p*NP was 1.66 min, the t_R of *p*NPX was 1.80 min, the t_R of xylose was 3.01 min and the t_R of xylobiose was 4.0 min as determined with the corresponding standards.

2.5. Kinetic studies

The kinetic parameters, K_m (Michaelis constant) and V (maximum velocity) were obtained by fitting the experimental data by non-linear regression to the Michaelis–Menten equation with a SIGMA PLOT 4.0 program. The data are presented in the figures as double-reciprocal plots in order to facilitate pattern recognition. Each point represents the mean of at least two experiments plus or minus the standard deviation (where error bars are not evident, they are within the size of the symbol).

Inhibition studies were carried out as indicated in the legends of the figures. The inhibition constant, K_i, was obtained from the linear re-plots of slopes (K_{is}) and or intercepts (K_{ii}) by a standard least-squares method. Parabolic re-plot was fitted to Eq. (2) according to Cleland [20]:

$$\text{slope} = a(1 + bI + cI^2) \quad (2)$$

where I is the inhibitor concentration and a, b and c are constants.

3. Results

β-Xylosidase activity was linear up to15 μg protein and up to 35 min with *p*NPX, MUX and xylobiose as substrates under the stated conditions. The optimum temperature for catalysis was 55°C, the optimum pH was 4.0 and the enzyme was stable at 55°C under the assay conditions [15]. The enzyme was not sensitive to changes in ionic strength up to 2 M NaCl.

3.1. Initial velocity studies

Initial velocity studies were carried out with xylobiose and two aryl β-xylosides: 4 methylumbelliferyl-β-D-xylopyranoside (MUX) and *p*-nitrophenyl-β-D-xylopyranoside (*p*NPX) as substrates. The hydrolytic reactions catalysed by β-xylosidase on them released

Table 1
Kinetic parameters of β-xylosidase[a]

Substrate	K_m (mM)	V (μmol/(min mg))	V/K_m	log P aglycone
Xylobiose	2.37 ± 0.72	47.69 ± 7.62	20.12	−4.26
*p*NPX	3.11 ± 0.61	3.33 ± 0.26	1.07	1.23
MUX	0.87 ± 0.21	8.2 ± 1.21	9.43	1.85

[a] The initial velocity study was carried out with 76 μg protein and 0.1–3 mM xylobiose, with 10.6 μg protein and 0.15–12 mM *p*-nitrophenyl-β-D-xylopyranoside (*p*NPX) or with 2.65 μg protein and 0.02–1 mM 4-methylumbelliferyl-β-D-xylopyranoside (MUX). Other conditions as in the standard assays with the same substrates. The log P (partition coefficient) of the aglycones was calculated by the fragmental constants method following a published procedure [23].

D-xylose plus an aglycone, either D-xylose, *p*-nitrophenol (*p*NP) or 4-methylumbelliferone (MU) according to:

xylobiose → xylose + xylose

*p*NPX → xylose + *p*NP

MUX → xylose + MU

No substrate inhibition was observed whatever the substrate and up to the highest concentration tested (not shown). The kinetic parameters are summarized in Table 1 where we can see that the highest catalytic efficiency (V/K_m) of the enzyme was obtained towards its natural substrate, xylobiose. The lowest K_m was found for MUX, the substrate whose aglycone (MU) is the most hydrophobic according to its calculated log P (see Table 1).

Kinetics towards *p*-nitrophenyl-α-L-arabinopyranoside (*p*NPA) could not be carried up since the hydrolytic activity of β-xylosidase was very low towards this substrate, about 200-times lower than the showed with xylobiose.

3.2. Product inhibition

Product inhibition was conducted to determine whether there is an obligatory order in the release of products. Xylobiose, the natural substrate, was discarded as the variable substrate since its hydrolysis gives two identical reaction products. MUX was also discarded given the low solubility in buffer of the aglycone MU. Therefore, *p*NPX was chosen as the variable substrate for product inhibition studies.

The inhibition by xylose (X) was competitive (Fig. 1). The slope re-plot versus inhibitor concentration fitted to a straight line (Fig. 1, inset) and the horizontal intercept of re-plot gave the inhibition constant $K_{is} = 1.69$ M. The lack of intercept effect in the inhibition by xylose suggests that xylose combines with the same enzyme form as the substrate, that is, the free enzyme (E) to form the complex E · X which in turn would decrease the E available to combine with the substrate, and thus, affect the slope.

The inhibition by *p*-nitrophenol (*p*NP) was non-competitive (Fig. 2). The intercept effect suggests *p*NP binds to an enzyme form other than the free enzyme. The re-plot of intercepts (i) is linear (Fig. 2, inset) and $K_{ii} = 46.58$ mM. The re-plot of slopes (s) is parabolic (Fig. 2, inset) suggesting there is mixed dead-end and product inhibition. According to theoretical considerations of Rudolph [21], the formation of a dead-end complex of the free enzyme

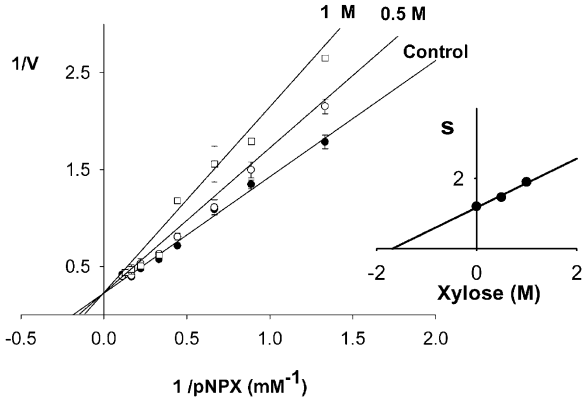

Fig. 1. Double-reciprocal plot of inhibition by D-xylose. Reciprocals of initial velocity in μmol/(min mg) were plotted vs. reciprocals of 0.75–9 mM *p*NPX. Each incubation contained 10.6 μg protein and 0 (control, ●), 0.5 M (○) or 1 M (□) D-xylose in a final volume of 1 ml. The release of *p*NP was measured at 400 nm. Other conditions as in the enzymatic standard assay with *p*NPX. Inset, slope re-plot vs. excess D-xylose.

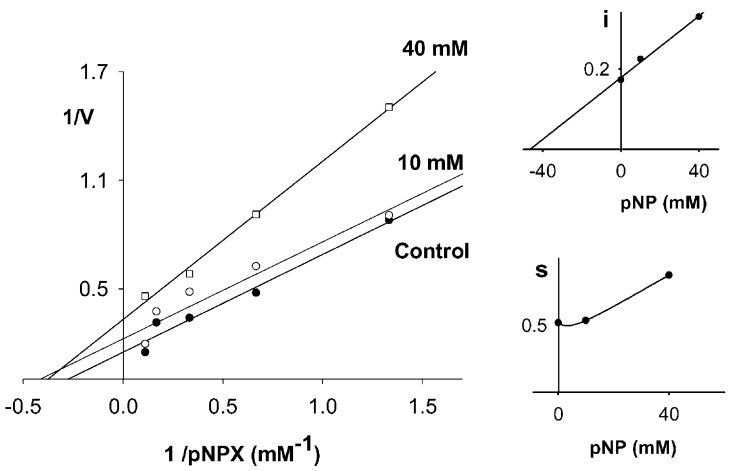

Fig. 2. Double-reciprocal plot of inhibition by *p*-nitrophenol. Each incubation contained 10.6 μg protein, 0.75–18 mM *p*NPX and 0 (control, ●), 10 mM (○) or 40 mM (□) *p*NP. The release of D-xylose was measured by HPLC. Units as in Fig. 1. Other conditions as described in Section 2. Inset, intercept (i) and slope (s) re-plots vs. inhibitor concentration.

with the product which causes an additional effect on slopes, can be inferred from the parabolic re-plot in Fig. 2 (inset). Since the secondary re-plots are defined by different functions, linear and parabolic, the double-reciprocals do not intersect at the same point (Fig. 2).

Product inhibition patterns by xylose and *p*NP allow us to asign tentatively a kinetic mechanism to the hydrolysis of *p*NPX by β-xylosidase. An Ordered Uni Bi mechanism is compatible [21] with the above results, *p*NP being the first product to leave the enzyme, followed by the transfer of xylose to water. In the proposed mechanism according to the nomenclature suggested by Cleland [22] (Scheme 1), xylose (X) as product would combine with the free enzyme (E) in competition with the substrate (*p*NPX). Moreover, *p*NP as product would add to the xylosyl-enzyme forming the complex (E·*p*NP·X), but also as dead-end inhibitor to the free enzyme (E) to form a dead-end complex (E · *p*NP) decreasing the enzyme form with which the substrate is combining and creating an additional slope effect.

3.3. Dead-end inhibition by D-glucono-1,5-lactone

Dead-end inhibition on *p*NPX hydrolysis was studied with D-glucono-1,5-lactone (GL) (Fig. 3). This is not a substrate, but resembles the reaction product (xylose). GL solutions in standard buffer were prepared and used within 30–60 min in kinetic assays. Polarimetric analysis of GL samples at 30 and 60 min after being dissolved gave 12.5% of the initial 160 mM GL and 11.4% of the initial 200 mM GL at 30 min and also at 60 min, indicating that mutarotation is achieved

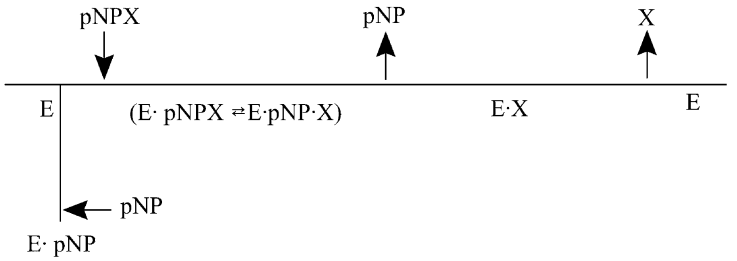

Scheme 1.

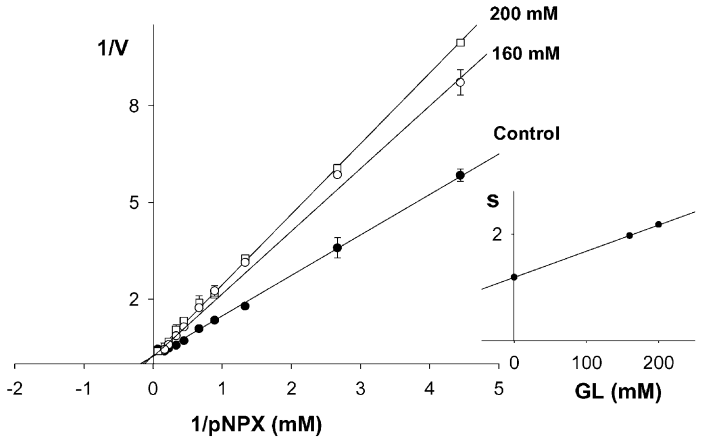

Fig. 3. Double-reciprocal plot of D-glucono-1,5-lactone addition on the *p*NPX kinetics. 10.6 μg protein were incubated with 0.225–15 mM *p*NPX and either 0 (control, ●), 160 mM (○) or 200 mM (□) D-glucono-1,5-lactone (apparent concentrations). Other conditions as described for the assay with *p*NPX. Units as in Fig. 1. Inset, slope re-plot vs. apparent inhibitor concentration.

speedily. However, the gluconic acid in the samples (the remaining percent), should also act as inhibitor since it has been described that the breakdown of the lactone ring of GL does not prevent the binding of the molecule to glycosidases, but only decreases it [5]. Therefore, to draw Fig. 3, we have taken the initial GL concentrations (apparent), regardless of the state of the lactone ring. The inhibition pattern in Fig. 3 is competitive since GL as product analog must combine with the free enzyme to form a dead-end complex (E·GL) which confirms the proposed mechanism [20]. The slope re-plot is linear (Fig. 3, inset) indicating that only one molecule of GL binds to free enzyme to form the complex whose dissociation constant can be calculated from the abscissa intercept of the re-plot (apparent $K_{is} = 241$ mM).

3.4. Alternative product study

In order to confirm again the proposed mechanism, Ordered Uni Bi, alternative product studies have been carried out [22]. The aglycone product of MUX hydrolysis, MU, has been used as alternative product on the *p*NPX hydrolysis by β-xylosidase. In the presence

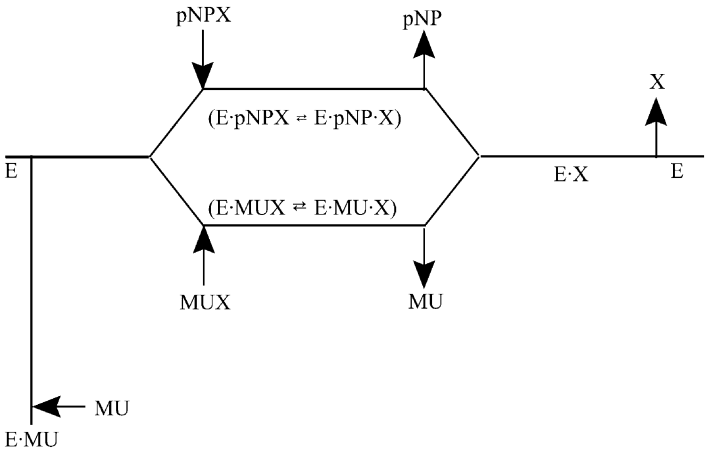

Scheme 2.

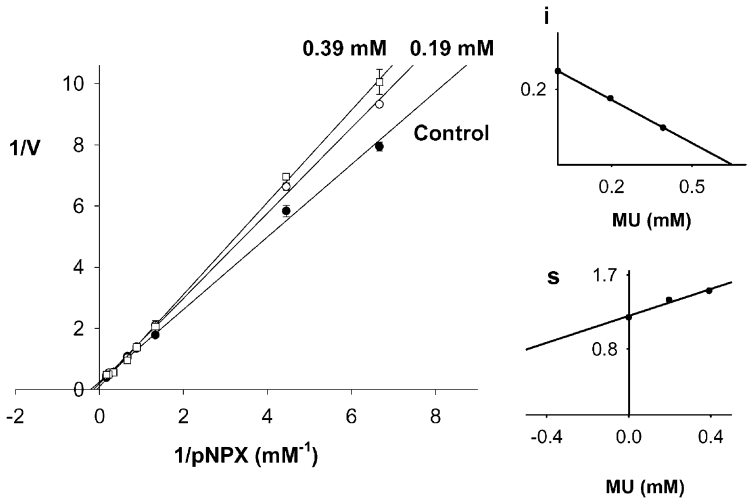

Fig. 4. Double-reciprocal plot of 4-methylumbelliferone effect on the *p*NPX kinetics. Incubation contained 10.6 μg protein, 0.15–6 mM *p*NPX and either 0 (control, ●), 0.19 mM (○) or 0.39 mM (□) 4-methylumbelliferone (MU). Other conditions as in the standard assay with *p*NPX except that routine controls of non-enzymatic *p*NPX hydrolysis also contained MU so that the absorbance at 400 nm due to the alternative product in the reaction media, was subtracted. Units as in Fig. 1. Inset, slope (s) and intercept (i) re-plots vs. MU concentration.

of MU, two reactions can take place:

$$p\text{NPX} \rightarrow p\text{NP} + \text{xylose} \quad \text{(a)}$$

$$\text{MU} + p\text{NPX} \rightarrow p\text{NP} + \text{MUX} \quad \text{(b)}$$

In consequence, the addition of MU would introduce an alternate sequence (b) to the hydrolysis of *p*NPX (a) as shows Scheme 2. The effect of MU when combining with (E × X) would be to divert the reaction flux from reaction (a) to (b).

Kinetics of *p*NPX hydrolysis in the presence of MU is depicted in Fig. 4 where we can observe a non-competitive pattern. According with reactions showed above, *p*NP is released in each catalytic cycle so that neither the first-order rate constant (V/K_m) nor the slope (K_m/V) should change so that an acompetitive pattern is expected, caused by the combination of MU with (E · X). However, since there is an slope effect in Fig. 4, the alternative product MU must also combine with free enzyme (E) to form a dead-end complex (E · MU), that is, MU competes with the substrate (see Scheme 2). The decrease of E available to the substrate would affect the first-order rate constant and so the slope. From the slope re-plot (Fig. 4, inset) can be obtained the dissociation constant of the dead-end complex ($K_{is} = 1.5$ mM).

The re-plot of intercepts is also linear (Fig. 4, inset), but shows activation. This effect is expected in the proposed mechanism when the unimolecular step for the MUX release from the central complex (E · MUX ⇌ E · MU · X) is faster than the breakage of (E · X) [20]. Therefore, the non-competitive pattern (slope linear, intercept linear) in the presence of MU as alternative product confirm the proposed mechanism and allows us to propose Scheme 2.

4. Discussion

β-Xylosidase from *Trichoderma reesei* QM 9414 catalyses the hydrolysis of its natural substrate, xylobiose, with the highest catalytic efficiency and of two aryl β-D-xylosides (*p*NPX and MUX). No substrate inhibition was found which indicates that neither ternary complexes of the type (substrate · enzyme · product) form nor two molecules of substrate adds to a pocket designed only for one. Moreover, β-xylosidase shows the highest affinity for the substrate whose aglycone is the most hydrophobic which points to the existence of residues involved in binding through interacting hydrophobically with the substrate. Studies of site-directed chemical modification and of protection

with the substrate, which are the content of an article in preparation, indicate the existence of an essential tryptophan which could be responsible of the interaction.

Inhibition, competitive by D-xylose and non-competitive by *p*NP, suggests that the enzyme catalyses the hydrolysis of *p*NPX through an Ordered Uni Bi mechanism with *p*-nitrophenol being the first product released. By analogy, when xylobiose is the substrate, the first product released should be the xylose whose anomeric carbon is free. Although there is no published evidence of proposed mechanisms for β-xylosidase, we have previously found that another glycosidase, β-glucosidase from *T. reesei*, follows also an Ordered Uni Bi mechanism [12].

Supporting evidence for the mechanism we propose comes from the studies with MU. This alternative product presumably undergoes the same catalytic events as the substrate, yet its presence gives rise to an alternative reaction pathway. It induces a non-competitive activation pattern in the hydrolysis of *p*NPX since acts also as a dead-end inhibitor when it combines with the free enzyme. Competitive patterns with non-lineal double-reciprocals were predicted by Huang [23] when the common product approach was employed and we have obtained competitive activation. With regard to dead-end inhibitors, GL is known to be a powerful inhibitor of different glycosidases given its structural similarity (when bound) with the glycosyl oxocarbenium ion intermediate, regardless of its state with the lactone ring open or closed since D-gluconic acid has been co-crystallized with a β-glucosidase [5]. It behaved in our system as an analog of xylose, combining with the free enzyme, causing competitive inhibition and confirming the role played by xylose as being the second substrate in leaving the enzyme.

If we assume the proposed mechanism, the high maximum velocity with xylobiose as substrate may indicate that the rate-limiting step of the hydrolytic reaction is different for xylobiose than for *p*NPX and MUX hydrolysis. So, whereas for *p*NPX and MUX hydrolysis, the release of the aglycone would probably be the rate-limiting step, the highly polar character of the first product in the xylobiose hydrolysis, xylose, would carry a change in rate-limiting step, so that now the overall process becomes independent of the nature of the leaving group.

The pH-dependence of the β-xylosidase kinetic parameters, which is the content of an article in preparation, point to the existence in the enzyme of two catalytic carboxyls. Although, we have detected no *trans*-xylosidation under our experimental conditions, there is published evidence about this process taking place [10]. These facts, together with the mechanism we propose, Ordered Uni Bi which implies the existence of an intermediate xylosyl · enzyme and taking into account the mechanisms that glycosidases follow [7], suggests that β-xylosidase from *T. reesei* hydrolyses β-xylosides by a double-displacement mechanism with retention of the anomeric carbon configuration.

Acknowledgements

This work has been financed by the Spanish CICYT (no. AMB 98-1043 C02-01).

References

[1] P. Biely, Trends Biotechnol. 3 (1985) 286–290.
[2] K. Poutanen, J. Puls, Appl. Microbiol. Biotechnol. 28 (1988) 425–432.
[3] M.L. Sinnot, Chem. Rev. 90 (1990) 1171–1202.
[4] A. White, D.R. Rose, Curr. Opinion Struct. Biol. 7 (1997) 645–651.
[5] J. Sanz-Aparicio, J.A. Hermoso, M. Martínez-Ripoll, J.L. Lequerica, J.J. Polaina, Mol. Biol. 275 (1998) 491–502.
[6] J.D. McCarter, G. Withers, Curr. Opinion Struct. Biol. 4 (1994) 885–892.
[7] S. Chiba, Biosci. Biotechnol. Biochem. 61 (1997) 1233–1239.
[8] E. Margolles-Clark, M. Tenkanen, N. Nakari-Setälä, M. Penttilä, Appl. Environ. Microbiol. 62 (1996) 3840–3846.
[9] A. Sunna, G. Antranikian, Crit. Rev. Biotechnol. 17 (1997) 39–67.
[10] M.C. Herrmann, M. Vrsanska, M. Jurickova, P. Biely, P. Kubiceck, Biochem. J. 321 (1997) 375–381.
[11] C. Acebal, M.P. Castillon, P. Estrada, I. Mata, E. Costa, J. Aguado, D. Romero, F. Jimenez, Appl. Microbiol. Biotechnol. 24 (1986) 218–223.
[12] P. Estrada, I. Mata, J.M. Dominguez, M.P. Castillon, C. Acebal, Biochim. Biophys. Acta 1033 (1990) 298–304.
[13] I. Mata, P. Estrada, R. Macarron, J.M. Dominguez, M.P. Castillon, C. Acebal, Biochem. J. 283 (1992a) 679–682.
[14] I. Mata, J.M. Dominguez, R. Macarron, C. Acebal, P. Estrada, M.P. Castillon, Ann. Quim. 88 (1992b) 365–368.
[15] M.J. Dueñas, P. Estrada, Biocatal. Biotrans. 17 (1999) 139–161.

[16] O.H. Lowry, N.J. Rosebrough, A.L. Farr, R.T. Randall, J. Biol. Chem. 193 (1951) 266–275.
[17] G.L. Miller, Anal. Chem. 31 (1959) 426–428.
[18] R.F. Boyer, Modern Experimental Biochemistry, 2nd Edition, Benjamin/Cunnings, Menlo Park, CA, 1993.
[19] The Merck Index, Edited by Merck & Co. Whitehouse Station, New York, 1996.
[20] W.W. Cleland, in: P. Boyer (Ed.), The Enzymes, Vol II, Academic Press, New York, 1970, pp. 30–33.
[21] F.B. Rudolph, Methods Enzymol. 63 (1979) 411–436.
[22] W.W. Cleland, Biochim. Biophys. Acta 67 (1963) 104–137.
[23] R.P. Schwarzenbach, P.M. Geschwend, D.M. Imboden, Environmental Organic Chemistry, Wiley, New York, 1993, pp. 124–156.